**Identifying Resource-rich Lunar Permanently Shadowed Regions: Table and Maps.** H.M. Brown, M.S. Robinson, and A.K. Boyd, Arizona State University, School of Earth and Space Exploration, PO Box 873603, Tempe AZ, 85287-3603 hbrown6@asu.edu

**Introduction:** Cold-trapped volatiles, including water-ice, in lunar Permanently Shadowed Regions (PSRs) could be a high priority resource for future space exploration [1]. Rates of supply and burial, distribution, and composition of PSR volatiles are poorly understood. Thus, amplifying the need to identify high priority PSR targets for focused exploration [1].

Current PSR observations from remote sensing instruments utilizing bolometric temperature, neutron spectroscopy, radar backscatter, 1064 nm reflectance, far-ultraviolet spectra, and near-IR absorption indicate surface and/or buried volatile deposits [2-8]; however, results from these datasets are not always correlated. We compared PSR observations [2-14] to identify sites that are most likely to host volatiles (Table 1, Figure 1).

The 10 largest-by-area PSRs at each pole were selected for study as well as 35 other smaller PSRs with high scientific interest [10-13]. For these 55 PSRs we compiled observations from published works [2-14] and scored them by volatile/resource potential (28 south pole, 27 north pole).

**PSR Volatiles Scoring:** For each PSR, each dataset [2-14] was categorized based on median and percent coverage values. Scores are split into three categories: consistent with volatiles (3; blue), conflicting observations or ambiguous results (2; yellow), and no coverage or inconsistent with volatiles (1; orange). Scores are weighted assuming equal value of importance for each dataset.

Lyman Alpha Mapping Project (LAMP) scores for the north pole were decreased by 1 due to a low signal-to-noise ratio (S/N) [7,11].

Lunar Orbiter Laser Altimeter (LOLA) reflectance and Mini-RF 13-cm and 4.3 cm radar Circular Polarization Ratio (CPR) values are positively correlated with steep slopes [5,6], making rendering scores sometimes problematic. For PSRs with median slopes >16°, LOLA and Mini-RF scores were decreased by 1.

Low S/N and image resolution in many Lunar Reconnaissance Orbiter Camera (LROC) Narrow Angle Camera (NAC) PSR images [15,16] may contribute to no positive detections of permafrost landforms, blocks <5 meters, or surface frost. However, ShadowCam, a future orbital instrument, aims to resolve this issue by providing high-resolution (1.7 meters/pixel) and high S/N (>100) PSR imaging [17].

*Ranking and Classification:* Total Rank was derived from the sum of the scored dataset categories for each PSR, with values ranging from 8 to 22. PSRs were classified by Total Rank: values >18 are considered consistent with volatiles, 13 to 17 are ambiguous, and PSRs with ranks <12 are considered inconsistent with volatiles. Dataset scores and Total Rank are listed in Table 1, which is sorted by Total Rank.

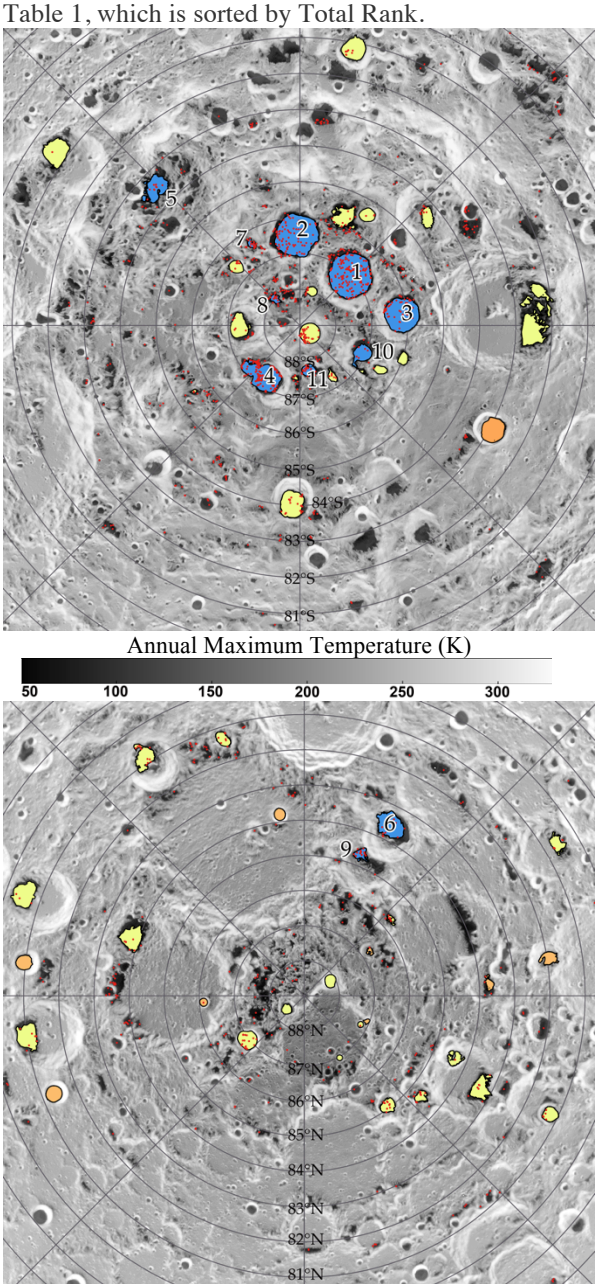


**Figure 1.** *South (top) and north (bottom) pole PSR volatile ranking thematic maps overlaying Diviner annual maximum bolometric temperature [1]. Blue PSRs are consistent with volatiles, while orange PSRs have no dataset coverage or are inconsistent with volatiles. PSRs in yellow have conflicting volatile detections or are ambiguous with volatiles. Red dots represent the intersection of surface volatile detections by*

*Moon Mineralogical Mapper (M3), LAMP, and LOLA [8]. PSRs that are consistent with volatiles, and therefore likely resource-rich, are labeled by Total Rank (1–11).*

**Conclusion:** Renewed interest in the Moon and recent water-ice detection in some PSRs [8] reinforces the need to identify high priority sites for lunar prospecting. The PSR Volatiles Ranking and corresponding maps summarize detections from lunar polar datasets, which allows for interpretation of resource-rich sites. The PSRs with the highest potential volatile economic grade and tonnage include: Shoemaker, Haworth, Faustini, Sverdrup, and Cabeus craters. Of these PSRs, Shoemaker has the highest median dataset values and most positive detection overlaps, displaying evidence for both patchy surface frost and buried ice deposits. Thus, we rank Shoemaker crater as having the highest priority for future surface exploration.

With the existing datasets, determining volatile resource grade and tonnage is not possible; however, our ranking of PSRs is a useful tool to guide future landed missions that can determine true resource potential (grade and tonnage).

**References:** [1] Arnold J.R. (1979), J. Geophys Res. 84:5659-5668. [2] Paige et al. (2010), 330, 6003. [3] Sanin et al. (2012), J. Geophys, Res., 117.E12. [4] Lawrence et al. (2006), J. Geophys, Res., 111.E8. [5] Spudis et al. (2013), J. Geophys, Res., 118.E10. [6] Glaser et al. (2014), Icarus, 243, 78-90. [7] Gladstone et al. (2012), J. Geophys. Res., 117.E12. [8] Li et al. (2018), PNAS., *115*(36), 8907-8912. [9] Mazarico et al. (2011), Icarus 211.2, 1066-1081. [10] Siegler et al. (2016), Nature, 531.7595, 480. [11] Hayne et al. (2015), Icarus, 255, 58-69. [12] Fisher et al. (2017), Icarus 292, 74-85. [13] Colaprete et al. (2010), Science, 330, 6003, 463-468 [14] Robinson et al. (2010), SSR, 150.1-4, 81-124. [15] Koeber et al. (2014), LPSC XLV, abs. #2811. [16] Mitchell et al. (2017), LPSC XLVIII, abs. #2481. [17] Robinson et al. (2018), LPV, abs. 2087.

| Crater Name | Longitude | Latitude | PSR Area ($km^2$) | Crater Diameter (km) | Median Slope (°) | Diviner Temp | LOLA Albedo | LAMP Albedo | Mini-RF CPR | LEND Neutron | LPNS Hydrogen | M3 NIR Ice Detection | LROC Albedo | Total Rank |
|---|---|---|---|---|---|---|---|---|---|---|---|---|---|---|
| Shoemaker | 45.3 | -88.0 | 1075.5 | 51.8 | 8.6 | | | | | | | | | 21 |
| Haworth | 357.9 | -87.5 | 1017.5 | 51.4 | 9.2 | | | | | | | | | 20 |
| Faustini | 84.1 | -87.1 | 663.9 | 42.5 | 11.4 | | | | | | | | | 20 |
| Sverdrup | 216.5 | -88.2 | 548.7 | 32.8 | 5.6 | | | | | | | | | 19 |
| Cabeus | 313.4 | -84.5 | 315.0 | 100.6 | 10.0 | | | | | | | | | 19 |
| Rozhdestvenskiy U | 153.1 | 84.6 | 397.2 | 44.1 | 9.4 | | | | * | | | | | 19 |
| Malapert Mountain (PSR is in a nearby crater) | 329.2 | -87.3 | 33.7 | not in crater | 10.9 | | | | | | | | | 19 |
| Haworth (PSR at flat terrain out of crater) | 317.1 | -88.9 | 44.2 | not in crater | 5.2 | | | | | | | | | 19 |
| Rozhdestvenskiy U (PSR is in a nearby crater) | 158.1 | 85.6 | 87.1 | 23.0 | 8.3 | | | | * | | | | | 18 |
| Slater | 114.8 | -88.1 | 183.2 | 25.1 | 5.6 | | | | | | | | | 18 |
| Sverdrup (PSR at flat terrain outside of crater) | 168.8 | -88.7 | 88.6 | 16.0 | 3.6 | | | | | | | | | 18 |
| Hermite A | 307.7 | 88.0 | 211.7 | 19.9 | 25.9 | | † | * | † | | | | | 17 |
| Shackleton | 128.2 | -89.6 | 233.6 | 20.9 | 30.3 | | † | | † | | | | | 17 |
| Sverdrup (PSR at flat terrain outside of crater) | 184.6 | -88.5 | 11.6 | not in crater | 3.5 | | | | | | | | | 17 |
| Slater (PSR at flat terrain outside of crater) | 126.3 | -87.8 | 10.6 | not in crater | 5.3 | | | | | | | | | 17 |
| Slater (PSR is out of the crater) | 147.5 | -88.3 | 50.6 | not in crater | 6.3 | | | | | | | | | 17 |
| Bosch | 131.1 | 86.7 | 34.0 | 19.5 | 8.0 | | | | * | | | | | 17 |
| Plaskett V | 120.9 | 81.5 | 137.3 | 44.6 | 13.3 | | | | * | | | | | 17 |
| Haworth (PSR at flat terrain out of crater) | 21.9 | -86.7 | 237.3 | not in crater | 6.6 | | | | | | | | | 17 |
| Shoemaker (PSR outside of crater) | 31.4 | -86.4 | 120.5 | 14.0 | 22.9 | | † | | † | | | | | 16 |
| Cabeus (PSR is outside of crater) | 312.5 | -87.5 | 101.8 | 11.0 | 27.2 | | † | | † | | | | | 16 |
| Shoemaker (PSR at flat terrain outside of crater) | 19.1 | -88.9 | 55.4 | not in crater | 5.7 | | | | | | | | | 16 |
| Shoemaker (PSR at flat terrain out of the crater) | 27.8 | -86.9 | 11.4 | not in crater | 6.9 | | | | | | | | | 16 |
| de Gerlache | 269.1 | -88.3 | 243.3 | 32.7 | 14.3 | | | | | | | | | 16 |
| Hermite A (PSR is out of the crater) | 291.1 | 88.0 | 20.0 | 5.0 | 15.6 | | † | * | † | | | | | 15 |
| Lenard | 251.5 | 84.8 | 292.0 | 47.7 | 11.5 | | | | * | | | | | 15 |
| Hinshelwood | 307.1 | 89.4 | 60.1 | 13.4 | 6.7 | | | | * | | | | | 15 |
| Sylvester | 278.3 | 82.0 | 317.3 | 59.3 | 12.0 | | | | * | | | | | 15 |
| Fibiger | 37.3 | 86.0 | 120.2 | 21.1 | 9.4 | | | | * | | | | | 15 |
| Rozhdestvenskiy K | 214.0 | 81.8 | 255.9 | 42.9 | 13.4 | | | | * | | | | | 15 |
| Plaskett (PSR is on the crater's wall) | 197.6 | 82.3 | 111.5 | 16.5 | 16.3 | | † | * | † | | | | | 14 |
| Nansen F (PSR is outside of crater) | 49.2 | 85.5 | 78.1 | 18.0 | 9.6 | | | * | | | | | | 14 |
| Faustini (PSR is out of the crater) | 107.8 | -86.9 | 68.5 | 22.0 | 6.7 | | | | | | | | | 14 |
| Amundsen | 91.0 | -83.5 | 439.2 | 103.4 | 10.4 | | | | | | | | | 14 |
| Slater (PSR is in a nearby crater) | 118.8 | -87.4 | 61.4 | 15.0 | 9.1 | | | | | | | | | 14 |
| Nobile | 49.9 | -85.3 | 139.3 | 79.3 | 10.6 | | | | | | | | | 14 |
| Wiechert J | 182.6 | -85.0 | 371.5 | 34.9 | 11.5 | | | | | | | | | 14 |
| Nansen A | 64.3 | 82.2 | 135.0 | 15.1 | 10.5 | | | | * | | | | | 14 |
| Cabeus B | 305.3 | -81.6 | 376.9 | 59.6 | 12.1 | | | | | | | | | 14 |
| Whipple | 119.5 | 89.1 | 86.9 | 14.5 | 28.8 | | † | * | † | | | | | 13 |
| Peary (PSR is on the crater's wall) | 63.0 | 88.1 | 20.1 | 7.0 | 24.1 | | † | * | † | | | | | 13 |
| Peary (PSR is on the crater's wall) | 92.8 | 89.6 | 10.0 | 5.5 | 22.0 | | † | * | † | | | | | 13 |
| Kocher/Sverdrup (PSR is outside of craters) | 238.1 | -86.5 | 10.3 | 7.9 | 6.6 | | | | | | | | | 13 |
| Malapert F | 11.1 | -82.1 | 300.5 | 31.0 | 14.3 | | | | | | | | | 13 |
| Nansen F | 62.5 | 84.3 | 253.0 | 62.0 | 11.0 | | | | * | | | | | 13 |
| Sylvester N | 291.3 | 82.3 | 154.6 | 20.0 | 29.2 | | † | * | † | | | | | 12 |
| Lovelace | 250.2 | 81.5 | 339.4 | 57.1 | 12.0 | | | | * | | | | | 12 |
| Rozhdestvenskiy W | 93.7 | 84.7 | 60.8 | 25.0 | 10.7 | | | | * | | | | | 11 |
| Rozhdestvenskiy (PSR is in crater) | 187.7 | 84.7 | 79.9 | 13.5 | 29.8 | | † | * | † | | | | | 11 |
| Rozhdestvenskiy N | 203.7 | 84.0 | 29.4 | 9.5 | 27.6 | | † | * | † | | | | | 11 |
| Rozhdestvenskiy W (PSR is out of the crater) | 123.9 | 87.7 | 23.7 | 14.0 | 5.1 | | | | * | | | | | 10 |
| Idelson L | 118.5 | -83.8 | 326.8 | 28.0 | 14.1 | | | | | | | | | 10 |
| Peary (PSR is on the crater's wall) | 67.7 | 88.0 | 16.2 | 7.1 | 11.8 | | | | * | | | | | 10 |
| Houssay | 98.7 | 82.9 | 123.0 | 31.4 | 16.8 | | † | * | † | | | | | 8 |
| Lovelace E | 263.2 | 81.9 | 140.0 | 21.7 | 17.0 | | † | * | † | | | | | 8 |
| Water-Ice and Volatiles Score of selected PSRs. | | | | | | Consistent with volatiles (3) | | | Ambiguous with volatiles (2) | | | Inconsistent with volatiles (1) | | |

**Table 1. Lunar PSR Volatiles Ranking Table.** Selection of PSRs based on scientific interest including the 10 largest PSRs for each pole. The table is based on 8 datasets: Diviner annual bolometric maximum temperature [1] and ice depth stability paleo/today [9] maps, LOLA 1064 nm reflectance [5], LAMP UV off/on band ratio [6], Mini-RF CPR [4], Lunar Exploration Neutron Detector (LEND) epithermal neutron flux [2], Lunar Prospector Neutron Spectrometer (LPNS) hydrogen abundance [3], M3 near-IR ice detections [7], and LROC NAC PSR imaging [13]. Scores are derived from dataset median values within each PSR, and total rank is the sum of dataset scores. The table is sorted by total rank. (†) in the LOLA and Mini-RF columns indicate reduced scores for high mean slope, and (*) in the LAMP column indicate reduced scores for low S/N in the north pole dataset.